Published in final edited form as:
J Eukaryot Microbiol. 2004 ; 51(6): 678–685.

An Analysis of the Microsporidian Genus *Brachiola*, with Comparisons of Human and Insect Isolates of *Brachiola algerae*

ANN CALI[a], **LOUIS M. WEISS**[b], and **PETER M. TAKVORIAN**[a]

[a]Department of Biological Sciences, 101 Warren Street, Smith Hall, Rutgers University, Newark, New Jersey 07102 USA

[b]Department of Medicine and Department of Pathology, Albert Einstein College of Medicine, Bronx, New York 10461 USA

Abstract

The genus *Brachiola* is the newest microsporidian genus established for a human infection with the type species being *B. vesicularum* in skeletal muscle. Subsequently, the microsporidium, *Nosema algerae*, identified from mosquitoes, was added to this genus because of morphological and physiological similarities. The present report illustrates a confirmed case of *Brachiola algerae* infecting skeletal muscle in a 56-year-old woman who was being treated for rheumatoid arthritis with immunosuppressive drugs. In the following study, these two human-infecting microsporidian species are ultrastructurally compared from human biopsy tissue. Additionally, *Brachiola algerae* from mosquitoes as reference *B. algerae*, was grown in athymic mice and compared to the human isolate in vivo, and in culture. *B. algerae* is morphologically identical in the host situations presented and different from *B. vesicularum* in human skeletal muscle. *B. algerae* has a consistently, slightly longer spore that typically contains one row of polar filament coils, while *B. vesicularum* typically contains two rows of polar filament coils and occasionally, one or three rows. In proliferative development, *B. vesicularum* forms protoplasmic extensions which do not occur on *B. algerae*, nor have they been reported on any other microsporidium. This report demonstrates that *B. vesicularum* and *B. algerae* are two different species of *Brachiola* that infect human skeletal muscle.

Keywords

Human myositis; opportunistic infections; Microspora; Microsporidia

The genus *Brachiola* was established for a microsporidium identified from an infection in human skeletal muscle (Cali et al. 1998). This genus was placed in the family Nose-matidae because of its shared developmental characteristics: diplokaryotic nuclei, developmental stages in direct contact with the host cell cytoplasm, the lack of plasmodial stages, and a disporous sporogony. The unique features of the genus *Brachiola* include a tolerance for temperatures of 37 °C, precocious thickened plasmalemma, a variety of plasmalemmal ornamentations and appendages. Additionally, the type species, *Brachiola vesicularum*, forms unique elongated developmental stages that produce protoplasmic extensions, often covered by the vesiculotubular appendages, Its spores are ovoid and measure 2.9 × 2 μm with the polar filament typically arranged in two rows, but one- and three-row arrangements also occur (Cali et al. 1998).

Corresponding Author: A. Cali—Telephone number: 973-353-5364; FAX number: 973-353-1007; anncali@andromeda.rutgers.edu.

Currently the genus contains four species: *B. vesicularum*, *Brachiola algerae*–previously *Nosema algerae* (Lowman, Takvorian, and Cali 2000), *Brachiola connori*–previously *Nosema connori* (Cali et al. 1998), and *Brachiola gambiae*–formerly *Nosema stegomyiae* (Weiser and Zizka 2004). All but *B gambiae* have been identified in humans.

When it was demonstrated that *N. algerae* could grow at elevated temperatures of 37 °C, in addition to having similar morphological and developmental features with the genus *Brachiola* (but lacking the protoplasmic extensions of the type species, *B. vesicularum*), reclassification was implicated. Molecular phylogenetic studies using the large subunit rRNA gene had indicated that *N. algerae* was an "out group" when compared to the *Nosema* type species (*N. bombycis*), suggesting that *N. algerae* did not belong in the genus *Nosema* (Baker et al. 1994); consequently, it was placed in the genus *Brachiola* (Lowman, Takvorian, and Cali 2000). Subsequently, Muller et al. (2000), while using another strain of *B. algerae*, stated that in no case was their *B. algerae* isolate located within the *Nosema*/*Vairimorpha* clade. Recently, Slamovits, Williams, and Keeling (2004) compared small subunit (SSU) rRNA sequence data of many microsporidia, including the *B. algerae* reference organism, and also demonstrated that it is distantly positioned relative to the *Nosema* type organism.

Brachiola algerae, originally isolated from mosquito larvae (Vavra and Undeen 1970), has been demonstrated to grow in many insect, mammalian cell cultures (including human), and the footpads, tail, and ears of mice (Lowman, Takvorian, and Cali 2000; Moura et al. 1999; Trammer et al. 1997; Undeen 1975; Undeen and Alger 1976; Undeen and Maddox 1973). However, it was not until recently that its tolerance for the mammalian body temperature of 37 °C was demonstrated in several types of cell culture (Lowman, Takvorian, and Cali 2000; Trammer et al. 1999; Visvesvara et al. 1999). Additionally, it has been isolated and identified from human eye scrapings (Visvesvara et al. 1999), and subsequently grown in SCID mice (Koudela et al. 2001). The present *B. algerae* (documented by PCR) biopsy material was obtained from human quadriceps muscle (Coyle et al. 2004) and is the first description of a human infection of *B. algerae* (HBa) in deep tissue. The purpose of the present report is to compare this new human isolate with what is known about *Brachiola* species. Specifically, the development of this organism in biopsy tissue is morphologically described, the development of *B. vesicularum* from another human biopsy is compared, and both are compared to the reference isolate of *B. algerae* (RBa) grown in mammalian cell culture and athymic mice, as well as the human isolate (HBa) grown in mammalian cell culture.

MATERIALS AND METHODS

In vitro growth of *Brachiola algerae*

The type organism of *Brachiola* (*Nosema*) *algerae* (Vavra and Undeen 1970) Lowman, Takvorian, and Cali 2000 used in these experiments was provided by Dr. A. Undeen from his original isolate and has been maintained in the Cali laboratory for several years. Since it is the type isolate, it will be referred to as the reference isolate (RBa). This organism was maintained in both rabbit kidney epithelial cells (RK13) cells and rat myoblast L6E9 cells at 32 °C in a 5% CO_2 environment. Both RK13 and L6E9 cells were grown to produce a confluent monolayer in 25 cm^2 flasks (Corning) at 37 °C, then transferred to 29 °C or 32 °C respectively, and infected with 10^6 spores of *B. algerae*. RK13 cells were maintained in Minimal Essential Media containing 7% fetal calf serum and 1% penicillin/streptomycin/amphotericin B (Invitrogen). L6E9 cells were maintained in Dulbecco's Minimal Essential Media (high glucose) containing 10% fetal calf serum and 1% penicillin/streptomycin. The human isolate of *B. algerae* (ATCC-PRA109) will be referred to as Hba. It was obtained

from a thigh muscle biopsy as previously described (Coyle et al. 2004) and maintained in L6E9 cells.

In vivo model of *Brachiola algerae* infection

Athymic nude mice (Balb/$c^{Nu/Nu}$) were obtained from the National Cancer Institute and housed in microisolator cages. Three athymic mice were inoculated subcutaneously at the base of their tails with 5×10^6 spores of the *B. algerae* mosquito reference isolate (RBa) that had been grown at 32 °C in RK13 cells. Two other athymic mice served as uninfected controls. Ten weeks post inoculation the mice were euthanized. Samples of spleen, liver, kidney, and tissue from the site of inoculation (i.e. skeletal muscle and sub-cutaneous fibrous tissue from the tail) were fixed in 0.1 M cacodylate-buffered 2.5% (v/v) glutaraldehyde, pH 7.2 for electron microscopy.

Electron microscopy

Biopsy tissues were fixed in 0.1 M cacodylate-buffered 2.5% (v/v) glutaraldehyde, pH 7.2. These were received as large cubes which were subsequently recut into several sub-blocks for transmission electron microscopy (TEM) using standard methods. Some tissue processed for light microscopy was received in wax tissue blocks, these were deparaffinized, hydrated, and postfixed in 2.5% (v/v) glutaralde-hyde and 1.0% (w/v) OsO_4 in 0.1 M cacodylate buffer, pH 7.2, then processed for electron microscopy. Tissue culture cells were fixed in 0.1 M cacodylate-buffered 2.5% (v/v) glutaraldehyde and then processed for TEM using standard methods. Thin sections were stained with uranyl acetate and lead citrate. The samples were observed using a Tecnai 12 TEM at the Rutgers University Electron Microscopy Facility.

Light microscopy

Muscle biopsy tissue received fresh was embedded on cork and snap frozen in an acetone/dry ice slurry. Cryostat sections were stained with hematoxylin and eosin (H&E) and Gomori trichrome stains. Additional muscle tissue was fixed in 10% (v/v) neutral buffered formalin, embedded in paraffin, sectioned, and stained with H&E and Wright-Giemsa using standard techniques.

RESULTS

Human quadriceps muscle biopsies containing *Brachiola algerae*

Light microscopy of Giemsa and H&E-stained sections revealed the presence of large masses of organisms within individual muscle cells (Fig. 1). Diplokaryotic nuclei were visible within some of these spores. Electron microscopic examination demonstrated the presence of the parasite stages in direct contact with the infected host cell cytoplasm (Fig. 2). These parasite cells were diplokaryotic and have the precociously thickened plasmalemma (Fig. 3) and vesiculotubular appendages, characteristic of the genus *Brachiola*. Clusters of organisms in different stages indicated that the parasite development was asynchronous (Fig. 4, 5), with proliferative, sporogonic, and spore stages all intermixed.

Many proliferative diplokaryotic cells were present in the infected host cell cytoplasm. However, cells containing two diplokaryotic pairs were not observed. Cells that appeared to have just divided may be seen as two abutted cells each containing a diplokaryon while cells that are elongated with an invagination in the middle (Fig. 5) appeared to be in early stages of cytokinesis. Additionally, proliferative cells containing DNA condensed into chromosomes in preparation for nuclear division were observed. These diplokaryotic nuclei (Fig. 6, 7) clearly indicate the presence of karyokinetic activity. Low-power micrographs revealed the presence of much dense material in the host cell cytoplasm, scattered around

the parasite cells (Fig. 5). This material is consistent with the appearance of the vesiculotubular appendage remnants as parasite cells mature. The proliferative stages had connections to this material on their plasmalemmal surface (Fig. 3, 6). However, as the sporogonic phase of development commenced, this material seemed to condense, become more dense, and break off (Fig. 8–10), becoming free in the host cell cytoplasm by the time the parasites sporulated (Fig. 11). As the percentage of sporulated cells increased within a host cell, the quantity of free, dense material also increased.

Sporoblasts may be identified by the increased density of their cytoplasm, the detachment of most of the vesiculotubular material from the now uniformly thicker cell surface, the irregular shape of the cells, and/or the presence of developing polar filament coils (Fig. 11).

The approximate size of fresh spores isolated from human host tissue was 4 × 2 μm. The elongated spores observed in the biopsy tissue sections viewed on the light microscope sometimes contained visible diplokarya (Fig. 1). Electron microscopic observations revealed the presence of a thick, dense exospore coat surrounding the thicker, lucent layer that contains the spore contents, including the plasmalemma, extrusion apparatus, and sporoplasm. These spores contained 8–11 polar filament coils in a single row surrounding the diplokaryon (Fig. 12, 13).

Human *Brachiola algerae* (HBa) isolate, grown in a rat muscle cell line (L6E9)

The human isolate grew rapidly and abundantly in this cell line. All stages of development were present in the undifferentiated rat muscle cells (Fig. 14, 15). The asynchronous nature of the parasite was obvious in low-power micrographs where all stages of the parasite could be seen in these heavily infected cells (Fig. 16). Intermixed among the sporoblasts and spores were large quantities of vesiculotubular remnants, which were attached to the surface of the proliferative cells (Fig. 17).

The spores were typical of *B. algerae* (Fig. 18), with 8–11 polar filament coils arranged in a single row. Fresh spores averaged 3.96 × 2.70 μm in size (± 0.025; N = 50).

The *Brachiola algerae* reference isolate (RBa), from mosquitoes, grown in athymic mice

Host cell cytoplasm from the mouse tail tissue contained all stages of parasite development (Fig. 19). The proliferative cells were decorated with the vesiculotubular structures typical of *Brachiola* (Fig. 20). The only elongated proliferative parasite cells observed were cells containing one diplokaryon, usually eccentrically positioned, and probably recently divided, or containing nuclei with condensed chromatin (Fig. 21). The sporoblastic cells were characterized by a more uniformly thickened plasmalemma, lacking most of the vesiculotubular surface structures, and possessing a denser cytoplasm than that present in earlier proliferative stages (Fig. 22). The vesiculotubular surface structures that were attached to the plasmalemma in those stages were now present as dense aggregates of material scattered around the parasite cells, in the host cell cytoplasm. The spores contained 9–10 polar filament cross-sections in a single row (Fig. 23).

DISCUSSION

The morphology and development of the microsporidium in deep muscle tissue from an infected patient conformed to the features of the RBa organism isolated from mosquitoes and grown in both RK13 cell culture (Lowman, Takvorian, and Cali 2000) and athymic mice. The human isolate, grown in rat-muscle cell culture, possessed all the stages and features observed in the biopsied tissue.

Development

Elongated cells with more than two diplokarya are not characteristic of any of the *B. algerae* isolates and were not observed in any of the material in this study, as karyokinesis and cytokinesis appear to be linked (Avery and Anthony 1983; Cali et al. 1998; Canning and Sinden 1973; Koudela et al. 2001; Lowman, Takvorian, and Cali 2000). In the biopsy tissue, dividing stages were hard to find. However, signs of active cell division were present: cells containing condensed chromatin were often observed, and infected muscle cells containing several proliferative stages interspersed with sporoblasts and spores indicated parasite proliferation. Cells that have probably just divided may appear as two abutted cells each, containing a diplokaryon, and the few cells that were elongated appeared to be in the early stages of cytokinesis. Cells containing condensed chromatin in their diplokaryotic nuclei also indicated the presence of karyokinetic activity.

Specializations of the parasite surface during development

A feature of the genus *Brachiola* (Cali et al. 1998; Lowman, Takvorian, and Cali 2000) and a characteristic of all *B. algerae* isolates presented here, are the unique cell surface manifestations. These include the precocious thickened plasmalemma and the formation of elaborate, dense vesiculotubular appendages, “blisters”, and ridges that are present during proliferative development. These appendages condense and detach from the plasmalemma during sporogony and sporogenesis, subsequently accumulating in the host cell cytoplasm as irregular dense bodies, leaving the parasite spore surface relatively smooth. The parasite surface characteristics appear to be consistent irrespective of the host situation in which the organism is placed (Avery and Anthony 1983; Cali et al. 1998; Canning and Sinden 1973; Koudela et al. 2001; Lowman, Takvorian, and Cali 2000; Vavra and Undeen 1970).

Spore morphology

The spores possess a thick electron-dense exospore coat over the lucent endospore. Mature spores average approximately 4 μm in size with 8–11 polar filament coils arranged in a single row, surrounding the diplokaryotic nuclei. These features are consistent with all the *B. algerae* material examined in this study; including the reference isolate grown in athymic mice, the human biopsy, and the human isolate grown in L6E9 cell culture. These observations are also consistent with most of the reports of *B. algerae* (Cali, Weiss, and Takvorian 2002; Canning and Sinden 1973; Koudela et al. 2001; Lowman, Takvorian, and Cali 2000).

Human muscle *Brachiola algerae* compared to other *B. algerae* isolates

The microsporidium observed in the biopsy material has the same morphological characteristics and developmental pattern that have been observed in the *B. algerae* reference species, originally isolated from larvae of the mosquitoes *Anopheles stephensi* and other *Anopheles* species (Avery and Anthony 1983; Canning and Sinden 1973; Vavra and Undeen 1970). Similarly, when the reference species, RBa, was inoculated and grown in mammalian cell culture (Lowman, Takvorian, and Cali 2000) and in athymic mice (this report), the infected cells contained the same morphological and developmental features typically observed in mosquito infections (Avery and Anthony 1983). Additionally, when spores were isolated from the muscle biopsy tissue (HBa isolate), and inoculated into rat-muscle cell culture (L6E9), they successfully infected the cells and produced the same developmental stages observed in mosquitoes infected with *B. algerae*. Further, the HBa isolate, is also consistent with the developmental pattern and parasite morphology of a *B. algerae* isolate (CDC: V404) obtained from infected human corneal scrapings and grown in SCID mice (Koudela et al. 2001).

Brachiola vesicularum

The original description of the genus *Brachiola* was based on the morphological characteristics and developmental pattern of another microsporidium observed in a biopsy from an infection of the quadriceps of a HIV-positive patient (Cali et al. 1998). The type species, *B. vesicularum*, contains a unique developmental entity (observed on elongated cells) identified as protoplasmic extensions, which are continuous with the cell cytoplasm and extend from the cell-like arms (Fig. 24, 25). These extensions branch, vary in both length and width, and possess the same types of vesiculotubular structures that are described in association with the surface of the other developing stages (Cali et al. 1998). These protoplasmic extensions may be very elaborate and protrude from the parasite cell proper for several micrometers into the host cytoplasm. The protoplasmic extensions have not been described in any other microsporidium and appear to be unique to *B. vesicularum*. The spores of *B. vesicularum* are ovoid, measuring approximately 2.9 × 2.0 μm, and contain 8–10 polar filament coils usually arranged in 2 rows but, 1–3 rows also occur (Fig. 26–28) (Cali et al. 1998). These spores are smaller than those of *B. algerae* by approximately 25%, and possess a polar filament with a different arrangement.

The light microscopic images of the biopsy material described in the present report, were reminiscent of the light image (Fig. 1) of the *B. vesicularum* infection described by Cali et al. (1998). Since the infection described in the current report was also an infection from a quadriceps biopsy of an immunologically impaired patient who had a fever, it was suspected to be a *B. vesicularum* infection. After our initial ultrastructural observations indicated that the current biopsy tissue contained a *Brachiola* infection, sections were examined extensively, looking for the occurrence of multiple rows of polar filament coils in the spores and the “protoplasmic extensions” on developmental stages, which would support identification of the species as *B. vesicularum*. Despite intensive efforts, they were never observed in the biopsy material. Additionally, examination of fresh spores from this material indicated that they were longer than spores of *B. vesicularum* by approximately 25%. Based on spore size, the lack of protoplasmic extensions, polar filament arrangement, and confirmation from PCR analysis (Coyle et al. 2004), it was determined that the new isolate (HBa) was, in fact, *B. algerae*. Thus, *B. vesicularum* and *B. algerae* are morphologically different while developing in the same host tissue (human muscle) and at similar temperature, under conditions of immune suppression.

The existence of one microsporidium species infecting both mosquitoes and man brings an important issue to the forefront. While mosquito-vectored diseases of humans have long been known, the existence of such a microsporidium has not, hereto-fore, been included in the organisms so considered. This brings an entire new set of human epidemiological issues into play.

Acknowledgments

The authors wish to thank Sharon Lewin, M.D. of St Luke's Roosevelt Hospital Center, New York City, NY and Luther V. Rhodes III, M.D. Lehigh Valley Hospital Allentown, PA for originally providing the biopsy tissues used in these studies, Mrs. Cyrilla Pau for technical assistance, and Christina M. Coyle, M.D. of Jacobi Medical Center, Bronx, NY and Lynn Garcia of LSG & Associates, Santa Monica, CA for facilitating the communication between the various laboratories involved with the Hba infection. Supported by NIH Grant A131788.

LITERATURE CITED

Avery SW, Anthony DW. Ultrastructural study of early development of *Nosema algerae* in *Anopheles albimanus*. J. Invert. Path. 1983; 42:87–95.

Baker MD, Vossbrinck CR, Maddox JV, Undeen AH. Phylogenetic relationships among *Vairimorpha* and *Nosema* species (Microspora) based on ribosomal RNA sequence data. J. Invert. Pathol. 1994; 64:100–106.

Cali A, Weiss LM, Takvorian PM. *Brachiola algerae* spore membrane systems, their activity during extrusion, and a new structural entity, the multilayered interlaced network, associated with the polar tube and the sporoplasm. J. Eukaryot. Microbiol. 2002; 49:164–174. [PubMed: 12043963]

Cali A, Takvorian PM, Lewin S, Rendel M, Sian CS, Wittner M, Tanowitz HB, Keohane E, Weiss LM. *Brachiola vesicularum*, n. g., n. sp., a new microsporidium associated with AIDS and myositis. J. Eukaryot. Microbiol. 1998; 45:240–251. [PubMed: 9627985]

Canning EU, Sinden RE. Ultrastructural observations on the development of *Nosema algerae* Vavra and Undeen (Microporida, Nosematidae) in the mosquito *Anopheles stephensi* Liston. Protistologica. 1973; 9:405–415.

Coyle C, Weiss LM, Rhodes LV, Cali A, Takvorian PM, F. BD, Visvesvara G, Xiao L, Naktin J, Young E, Gareca M, Calasante G, Wittner M. Fatal myostitis due to the micro-sporidian *Bachiola algerae*, a mosquito pathogen. N. Engl. J. Med. 2004; 351:42–47. [PubMed: 15229306]

Koudela B, Visvesvara GS, Moura H, Vavra J. The human isolate of *Brachiola algerae* (Phylum Microspora): development in SCID mice and description of its fine structure features. Parasitology. 2001; 123:153–162. [PubMed: 11510680]

Lowman PM, Takvorian PM, Cali A. The effects of elevated temperature and various time-temperature combinations on the development of *Brachiola (Nosema) algerae* n. comb. in mammalian cell culture. J. Eukaryot. Microbiol. 2000; 47:221–234. [PubMed: 10847338]

Moura H, da Silva A, Moura I, Schwartz DA, Leitch G, Wallace S, Pieniazek NJ, Wirtz RA, Visvesvara GS. Characterization of *Nosema algerae* isolates after continuous cultivation in mammalian cells at 37 °C. J. Eukaryot. Microbiol. 1999; 46:14S–16S. [PubMed: 10519228]

Muller A, Trammer T, Chioralia G, Seitz HM, Diehl V, Franzen C. Ribosomal RNA of *Nosema algerae* and phylogenetic relationship to other microsporidia. Parasitol. Res. 2000; 86:18–23. [PubMed: 10669131]

Slamovits CH, Williams BAP, Keeling PJ. Transfer of *Nosema locustae* (Microsporidia) to *Antonospora locustae* n. comb. based on molecular and ultrastructural data. J. Eukaryot. Microbiol. 2004; 51:207–213. [PubMed: 15134257]

Trammer T, Chioralia G, Maier WA, Seitz HM. In vitro replication of *Nosema algerae* (Microsporidia), a parasite of anopheline mosquitoes, in human cells above 36 °C. J. Eukaryot. Microbiol. 1999; 46:464–468. [PubMed: 10519213]

Trammer T, Dombrowski F, Doehring M, Maier WA, Seitz HM. Opportunistic properties of *Nosema algerae* (Microspora), a mosquito parasite, in immunocompromised mice. J. Eukaryot. Microbiol. 1997; 44:258–262. [PubMed: 9183715]

Undeen AH. Growth of *Nosema algerae* in pig kidney cell cultures. J. Protozool. 1975; 22:107–110. [PubMed: 235022]

Undeen AH, Alger NE. *Nosema algerae*: infection of the white mouse by a mosquito parasite. Exp. Parasitol. 1976; 40:86–88. [PubMed: 950003]

Undeen AH, Maddox JV. The infection of non-mosquito hosts by injection with spores of the Microsporidian *Nosema algerae*. J. Invert. Pathol. 1973; 22:258–265.

Vavra J, Undeen AH. *Nosema algerae* n. sp. (Cnidospora, Microsporida) a pathogen in a laboratory colony of *Anopheles stephensi* Liston (Diptera, Culicidae). J. Protozool. 1970; 17:240–249. [PubMed: 4915459]

Visvesvara GS, Belloso M, Moura H, da Silva A, Moura I, Leitch G, Schwartz DA, Chevez-Barrios P, Wallace S, Pieniazek NJ, Goosey J. Isolation of *Nosema algerae* from the cornea of an immunocompetent patient. J. Eukaryot. Microbiol. 1999; 46:10S. [PubMed: 10519226]

Weiser J, Zizka Z. *Bachiola gambiae* sp. n. the Microsporidian parasite of *Anopheles gambiae* and *A. melas* in Liberia. Acta Protozool. 2004; 43:73–80.

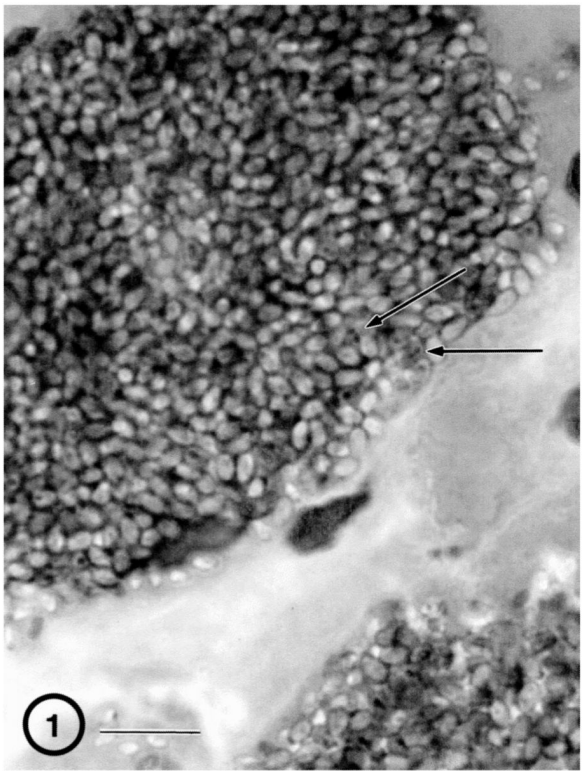

Fig. 1.
H&E-stained section of quadriceps muscle biopsy. A large cluster of organisms is present within the cytoplasm of the sarcosome. Diplokaryotic nuclei (arrows) are visible in some of the parasite cells. Bar = 10 μm.

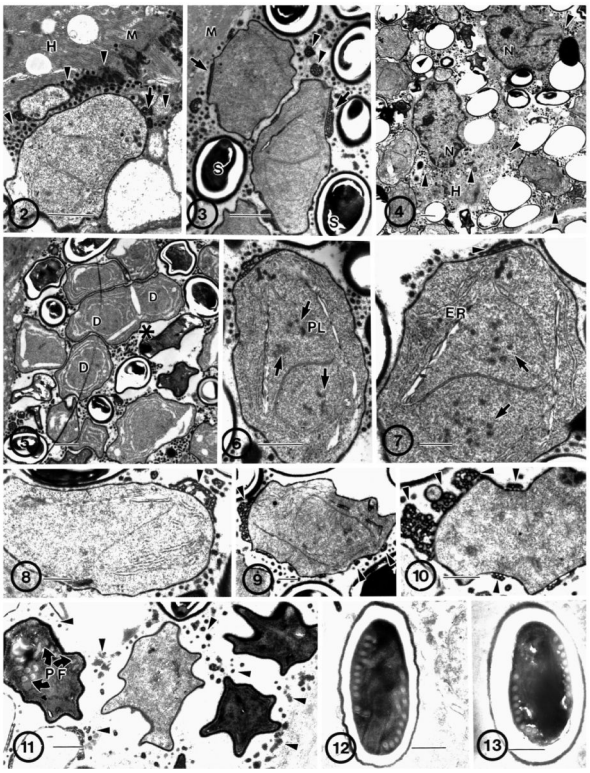

Fig. 2–13.

Electron microscopic overview of infected human muscle biopsy tissue containing developmental stages of the microsporidial parasite, *Brachiola algerae* (Hba). **2**. Early proliferative stages of the parasite in direct contact with the host muscle-cell cytoplasm (H). Note the presence of vesiculotubular appendages (arrow) attached to the parasite thickened plasmalemma, forming many dense bodies (arrowhead) in the host cytoplasm surrounding the parasite cells and abutting the host myofilaments (M). Bar = 1 μm. **3**. Diplokaryotic proliferative parasite cells and spores (S). Note the attachment of the vesiculotubular appendages (arrows) to the proliferative cells but not to the spores. Dense appendage material is present in the space between parasite cells (arrowheads). Bar = 1 μm. **4**. Low-power electron micrograph of clustered parasites in host cell cytoplasm (H). Host nuclei (N) and cytoplasm in direct contact with parasite cells and dense vesiculotubular appendage material (arrowheads) scattered throughout host cytoplasm. Note the lack of myofilaments between parasite cells. Bar = 1 μm. **5**. All parasite stages are present and intermixed, an indication of asynchronous development. Cytokinesis and karyokinesis are linked, resulting in individual organisms containing one diplokaryon (D) or two with indications of cell division (*). Bar = 1 μm. **6**. Proliferative cell containing a diplokaryon with condensed chromatin (arrows) and a spindle plaque (PL), indicating karyokinetic activity. Bar = 1 μm. **7**. Proliferative cell containing a diplokaryon with condensed chromatin (arrows), extensive ER, and attached dense vesiculotubular appendages (arrowhead). Bar = 0.5 μm. **8–10**. Sporonts. Note the change in appearance of the appendages (arrowhead) to clumps of dense material detaching from the plasmalemma. **8**. Early sporont. Note the relatively lower cytoplasmic density when compared to the other two. Bar = 0.5 μm. **9**. Note the presence of condensing chromatin in the sporont nucleus; it indicates the disporous nature of this parasite. Bar = 0.5 μm. **10**. Note the abundance of dense vesiculotubular appendage material (arrowhead) in the process of being sloughed off the plasmalemma as it becomes more homogeneously dense. Bar = 0.5 μm. **11**. Four sporoblasts with homogeneously thickened plasmalemma (after last cell division) and lacking attached appendages visible in the

surrounding cytoplasm (arrowheads). Note the presence of the forming polar filament (PF). Bar = 0.5 μm. **12–13**. Typical spores of *B. algerae* with 9–11 polar filament coils. **12**. Early activated spore. Note the translocation of some polar filament coils. Bar = 0.5 μm. **13**. Mature resting spore. Bar = 0.5 μm.

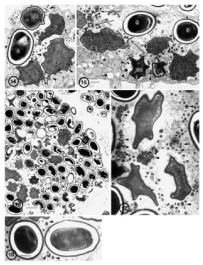

Fig. 14–18.

Human (Hba) isolate of *Brachiola algerae* grown in rat muscle (L6E9) cell line. **14**. Diplokaryotic proliferative (P) and sporogonic parasite cells, including sporonts (SP), sporoblast (SB), and spore (S) cells in direct contact with cell cytoplasm (H). Note the presence of detached appendage material (arrowheads) in the surrounding cytoplasm. Bar = 0.5 μm. **15**. Proliferative (P) and sporogonic parasite cells. Appendages (arrows) are attached to the surface of proliferative cells and the spores (S) and sporoblasts (SB) have a uniformly thick surface coating that lacks appendages, ridges or general irregularities. Detached appendage material (arrowheads) is clustered in the surrounding cytoplasm. Bar = 0.5 μm. **16**. Low power of infected host cell demonstrating the abundance of parasites filling the entire cell. Note the presence of all stages of development and the presence of dense appendage material scattered in the host cell cytoplasm. Bar = 10 μm. **17**. Sporoblasts containing forming polar filaments. Large clusters of detached appendage material (arrowheads) are in the surrounding cytoplasm. Bar = 0.5 μm. **18**. Spores. Mature elongate spore containing approximately 9–10 coils of polar filament arranged in a single row surrounding diplokaryotic nuclei. Bar = 1 μm.

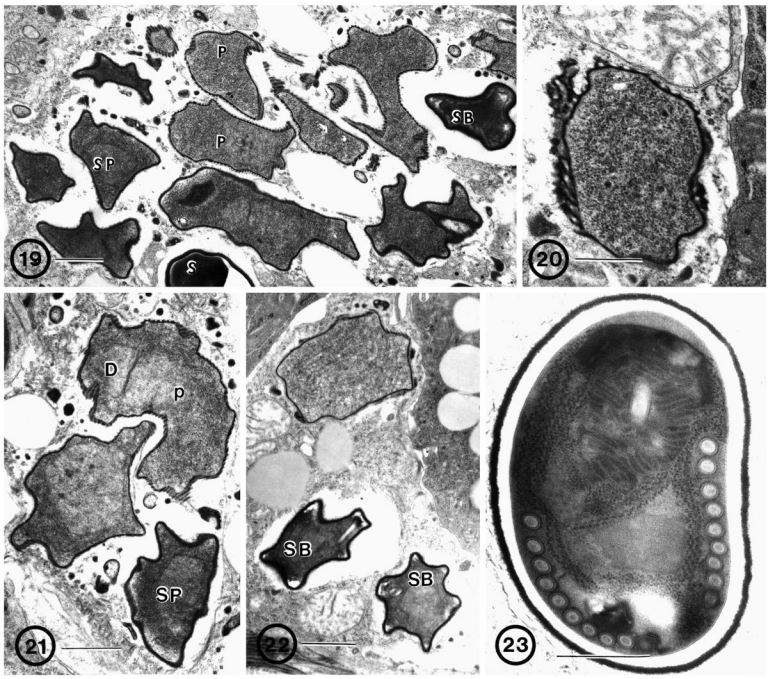

Fig. 19–23.

Reference isolate of *B. algerae* grown in athymic mice. **19**. Infected cell from the tail of the mouse. All parasite stages are present: diplokaryotic proliferative (P) and sporogonic parasite cells, including sporonts (SP), sporoblast (SB), and spore (S) cells in direct contact with cell cytoplasm. Note the difference in cell surface structure between early and late stages. Bar = 1 μm. **20**. Proliferative cell with thickened plasmalemma, appendages, and ridges. Bar = 0.5 μm. **21**. Elongated proliferative cell (P) with an eccentrically positioned diplokaryon (D). Note the difference in cytoplasmic density between the proliferative and sporont stages (SP). Bar = 1 μm. **22**. Two sporoblasts (SB) with homogeneously dense cell surfaces, denser cytoplasm, and the early stages of polar filament formation. Compare with proliferative cell above. Bar = 1 μm. **23**. Mature spore with 9–10 coils of the polar filament in a single row. Note the presence of a uniformly dense exospore coat. Bar = 0.5 μm.

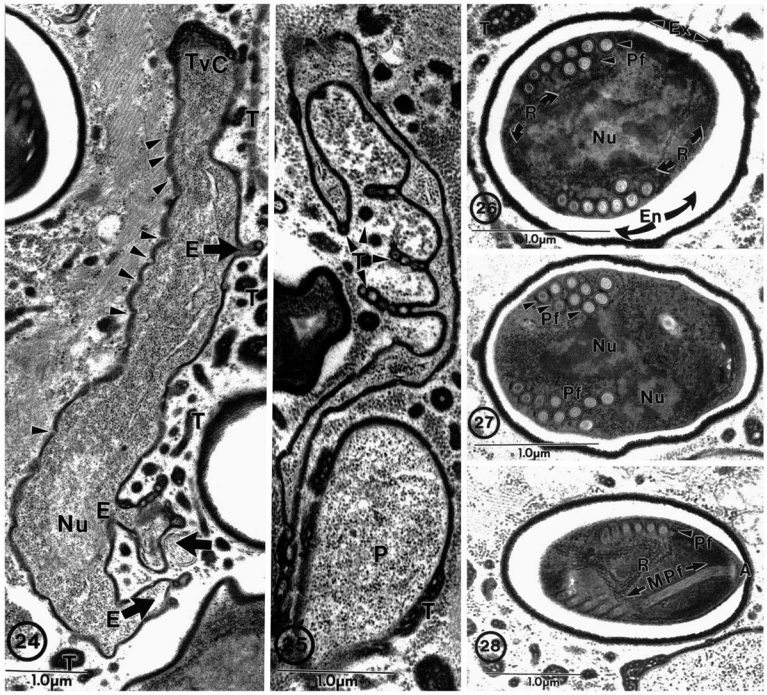

Fig. 24–28.

Brachiola vesicularum from human skeletal muscle biopsy. **24**. Proliferative cell with three protoplasmic extensions (E) projecting from the cell (broad arrows). Vesiculotubular appendages (T) associated with elongated cell and protoplasmic extensions. Note the nucleus (Nu), dense plasmalemma (arrowheads), and vesiculotubular cap (TvC) on the end of the parasite cell. **25**. Example of elaborate nature of protoplasmic extensions with associated vesiculotubular appendages (T) next to a proliferative (P) cell. **26**. Section through a spore illustrating the most common polar filament arrangement observed: nine cross-sections of an anisofilar polar filament (PF) coil arranged in two rows with two to three narrower diameter cross-sections. Spore structures include dense accumulations of ribosomes (R), nuclei (Nu), lucent endospore (En), and dense exospore (Ex) with some appendage material still attached. **27**. Spore containing ten polar filament (Pf) cross-sections clustered into three rows (arrowheads). **28**. Section through anterior anchoring disc complex (A) of the polar filament (Pf) illustrating its anterior manubroid (Mpf) portion and the cross-sections arranged in a single row. Note the presence of numerous ribosomes (R) inside the spore and the clusters of vesiculotubular material in the host cell cytoplasm. Bar = 1 μm. (All figures on this plate taken from Cali et al. (1998) with permission).